

1 Rethinking the deployment of static chambers for CO₂ flux 2 measurement in dry desert soils

3 Nadav Bekin, Nurit Agam

4 ¹Blaustein Institutes for Desert Research, Ben-Gurion University of the Negev, Sede-Boqer Campus, 84990, Israel

5 *Correspondence to:* Nurit Agam (agam@bgu.ac.il)

6 **Abstract.** The mechanisms underlying the soil CO₂ flux (Fs) in dry desert soils are not fully understood. To better
7 understand these processes, we must accurately estimate these small fluxes. The most commonly used method,
8 static chambers, inherently alter the conditions that affect the flux and may introduce errors of the same order of
9 magnitude as the flux itself. Regional and global assessments of annual soil respiration rates are based on
10 extrapolating point measurements conducted with flux chambers. Yet, studies conducted in desert ecosystems
11 rarely discuss potential errors associated with using static chambers in dry and bare soils. We hypothesized that a
12 main source of error is the collar protrusion above the soil surface. During the 2021 dry season, we deployed four
13 automated chambers on collars with different configurations in the Negev Desert, Israel. Fs exhibited a repetitive
14 diel cycle of nocturnal uptake and daytime efflux. CO₂ uptake measured over the conventionally protruding
15 collars was significantly lower than over the collars flushed with the soil surface. Using thermal imaging, we
16 proved that the protruding collar walls distorted the ambient heating and cooling regime of the topsoil layer,
17 increasing the mean surface temperatures. Higher soil temperatures during the night suppressed the flux driving
18 forces, i.e., soil-atmosphere CO₂ and temperature gradients, ultimately leading to an underestimation of up to
19 50% of the actual Fs. Accordingly, the total daily CO₂ uptake by the soil in the conventionally deployed collars
20 was underestimated by 35%. This suggests that desert soils are a larger carbon sink than previously reported and
21 that drylands, which cover approximately 40% of Earth's terrestrial surface, may play a significant role in the
22 global carbon balance.

23 1 Introduction

24 Soil respiration, i.e., the carbon dioxide (CO₂) efflux from the soil to the atmosphere, is among the largest
25 components of the carbon balance in terrestrial ecosystems, contributing approximately 60 PgC to the atmosphere
26 every year (Houghton, 2007). In arid and semi-arid environments, soil respiration is mostly considered to be
27 restricted to short pulses of increased moisture availability from rainfall events, during which microbial metabolic
28 activity increase rapidly, followed by long periods of desiccation and low to negligible soil respiration rates (Cable
29 et al., 2008; Austin et al., 2004). In the last two decades, studies carried out in several deserts have challenged this
30 paradigm, reporting a diel course of CO₂ exchange ~~during dry periods~~, consisting of nocturnal CO₂ uptake and
31 daytime efflux (Ball et al., 2009; Sagi et al., 2021; Lopez-Canfin et al., 2022). Researchers usually attribute this
32 diel cycle to changes in soil temperatures and soil air pressure that leads to cycles of expansion/contraction of soil
33 air, following the ideal gas law (Yang et al., 2020). These cycles change the surface CO₂ concentration and may
34 generate a soil-atmosphere pressure gradient (Ganot et al., 2014), both driving forces for soil CO₂ flux (F_s).
35 Another explanation is based on Henry's Law. It states that diurnal fluctuations of soil temperatures change the
36 solubility of soil CO₂ in water films, which changes the concentration of gaseous CO₂ in soil pores, leading to the
37 exchange of CO₂ between the soil and the atmosphere by diffusion (Fa et al., 2016). In saline/alkaline soils, this
38 process is thought to cause a diel cycle of calcium carbonate (CaCO₃) precipitation/dissolution, which enhances
39 F_s (Hamerlynck et al., 2013; Fa et al., 2016). Yet, the factors controlling F_s in desert soils and the partitioning
40 between them are still under debate.

41 Furthermore, the ability to accurately estimate the soil CO₂ flux in desert soils at the very dry-end is controversial
42 due to the potential for measurement-induced modifications to soil and atmospheric conditions that can introduce
43 errors of the same order of magnitude as the flux being measured. This problem is exacerbated when using static
44 chambers to measure flux, as the chambers inherently alter the conditions that affect the flux (Pumpanen et al.,
45 2010 ; Parkin et al., 2012). During efflux, CO₂ concentration in the chamber builds up, decreasing the diffusion
46 gradient between CO₂ in the soil pores and the chamber headspace, thereby altering CO₂ concentration within the
47 top soil layer and reducing the flux (Pumpanen et al., 2004). Artificial changes in air pressure within the chamber
48 headspace compared to the ambient atmosphere are another source of error (Bain et al., 2005; Lund et al., 1999).

49 There are additional sources of errors associated with the chamber-soil contact method (Ngao et al., 2006; Baram
50 et al., 2022). Flux chambers are typically deployed on a collar (i.e., PVC pipe) that is inserted into the soil, with
51 the upper 3-5 cm of the collar protruding above the soil surface to allow for chamber deployment. This practice
52 modifies the soil surface temperature by shading a portion of the measured surface area. The non-representative
53 soil surface temperature results in modified heat exchange between the soil and the atmosphere, as well as a
54 modified soil temperature profile (Ninari and Berliner, 2002). Soil microbial and physical processes that drive F_s
55 are susceptible to changes in soil temperature (Cable et al., 2011), and thus shading the soil surface can lead to
56 errors in F_s measurements. These errors may intensify in high-latitude cold deserts, in which the low angle of
57 insolation will dictate a larger shaded surface area for longer periods during the day. F_s was shown to be
58 particularly affected by fluctuations in soil temperatures in cold deserts (Parsons et al., 2004; Ball et al., 2009).

59 While these effects are likely minimal in temperate, vegetated areas, they could be significant in bare soil, partly
60 because fluctuations in surface temperatures are not regulated by vegetation cover as in humid environments.
61 Desert soils also have lower specific heat capacity than soils in humid environments due to lower water content

62 (Hillel, 1998). The lower water content also means that a larger portion of the available energy is invested in soil
63 heating rather than stored as latent heat during evaporation (Brutsaert, 1982). However, studies using static
64 chambers in desert ecosystems rarely discuss potential errors associated with the unique characteristics of desert
65 soils. Moreover, to our knowledge, the effect of collar height above the surface on soil surface temperature and,
66 consequently, on F_s was never studied.

67 Under dry soil conditions, the depth to which the collar is inserted can also significantly influence the flux
68 measurements. The ideal insertion depth is debatable, as both shallow and deep collar insertion depths can lead to
69 errors, depending on climate and soil conditions. Inserting the collar to a shallower depth than the depth to which
70 feedback from the chamber still affects gas concentrations may result in lateral diffusion, leading to
71 underestimation of the vertical flux (Healy et al., 1996). However, insertion depth of only 2.5 cm and a
72 measurement period of 10 minutes will reduce this underestimation to 1% for a soil with air-filled porosity of 0.3
73 $\text{m}^3 \text{m}^{-3}$ (Hutchinson and Livingston, 2001). Hence, for short measurement periods (common today) and soils with
74 low effective diffusivity, errors resulting from lateral diffusion may be insignificant. With current static chamber
75 systems, even small F_s measured in dry desert soils can be accurately quantified with much shorter measurement
76 periods of only 1-2 minutes (Yang et al., 2022), thus overcoming a significant drawback of the shallow collars.
77 Deep collar insertion, on the other hand, can lead to either overestimation or underestimation of the flux by
78 generating vertical mass flow of air along the collar walls or by facilitating root cutting, respectively (Heinemeyer
79 et al., 2011). Still, in most studies, collars are inserted to a depth of ~5-10 cm into the soil and, in some cases, to
80 a depth of 30-60 cm, while more than a third of all authors fail to report the collar insertion depth (Rochette and
81 Eriksen-Hamel, 2008; Cable et al., 2011; Fa et al., 2018; Jian et al., 2020; Sagi et al., 2021; Yang et al., 2022).

82 In this paper, we aimed to investigate the effect of collar height above the soil surface and collar depth of insertion
83 on F_s in a dry bare desert soil. Given the small fluxes in these conditions, and the fact that regional and global
84 assessments of annual soil respiration are based on extrapolating point measurements conducted with flux
85 chambers (Jian et al., 2020), minimizing measurement errors associated with the collar deployment technic is
86 critical. Arid and semi-arid regions, which comprise approximately 40% of Earth's terrestrial surface, constitute
87 the largest uncertainty on mean annual soil respiration estimations (Stell et al., 2021). Improving the accuracy of
88 F_s measurements in desert environments is essential for enhancing our understanding of the terrestrial carbon
89 balance and our ability to predict climate change.

90 **2 Materials and Methods**

91 **2.1 Research site**

92 The study was carried out at the Wadi Mashash Experimental farm in the Northern Negev, Israel (31°04'14''N,
93 34°51'62''E; 360 m.a.s.l; 65 km SE of the Mediterranean Sea). The climate in the research site is arid, with an
94 average annual rainfall of 116 mm (IMS, 2021), occurring between October and April. The daily mean maximum
95 and minimum temperatures for January (winter) are 15.9 C° and 8.0 C°, respectively, while those for August
96 (summer) are 33.3 C° and 20.7 C°. During the summer season, the prevailing wind direction is NW due to the sea
97 breeze carrying water vapor from the Mediterranean Sea inland. The sea breeze reaches its peak at a wind speed
98 of 7 m s^{-1} (at 10 m height) in the afternoon. The research is located on a largely bare plain of sandy-loam loess

99 soil (72.5% sand, 15% silt and 12.5% clay), partly covered by a biological soil crust over a thin physical crust,
100 with dry annual grasses and Shrubs.

101

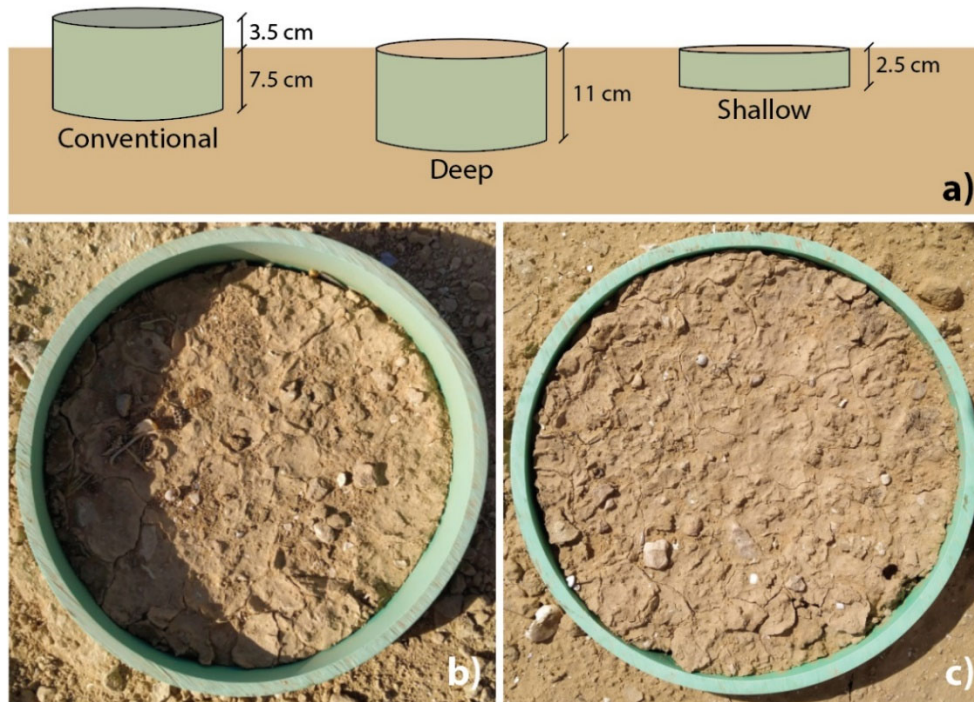
102 **2.2 Meteorological measurements**

103 Air temperature and relative humidity (100K6A1A, BetaTherm, USA) were monitored along with wind speed
104 and direction as part of an eddy-covariance system (IRGASON, Campbell Scientific Inc.). Air temperature was
105 measured at 5-second intervals and averaged over 15-minute periods. Wind speed and direction were determined
106 from high-frequency measurements of 3D wind speed taken at 20 Hz intervals, then averaged over 30-minute
107 periods and stored in a data logger (CR6, Campbell Scientific Inc.). Net radiation was measured at a height of 2.4
108 m using a 4-component net radiometer (SN-500-SS, Apogee instrument Inc, USA) at 10-second intervals,
109 averaged over 15-minute periods, and stored in a data logger (CR5000, Campbell Scientific Inc.).

110 **2.3 Soil CO₂ flux measurements**

111 We measured F_s using a non-dispersive Infrared Gas Analyzer with a range of 0-20,000 ppm and an accuracy of
112 1.5% of reading. The analyzer was connected to four automated non-steady-state chambers (LI 8100A- 104C, LI-
113 COR, Lincoln, USA). The chambers were closed on a pre-inserted collar every 30 minutes for a measurement
114 period of 60 seconds, with a 10-second dead band period to allow homogeneous air mixing within the system.
115 Each measurement started with a 90-second pre-purge and ended with a 45-second post-purge period.

116 We deployed the chambers on three types of collars (i.e., treatments): (1) The conventional type (CONV) - an 11
117 cm long collar, inserted 7.5 cm into the soil, leaving 3.5 cm of collar above the soil surface (Fig. 1); (2) The deep
118 type (DEEP) - an 11 cm long collar completely inserted into the soil, leaving the top of the collar flush with the
119 soil surface; and (3) The shallow type (SHAL) - a 2.5 cm long collar completely inserted into the soil, with the
120 top of the collar flush with the soil surface. Three collars from each type (1-3) were inserted into the soil two
121 months before measurements started. All collars had an inner diameter of 20 cm.



122
123 **Figure 1: a) The three types of collars used in this experiment. b) Photo of a conventional (CONV) collar. c) Photo of**
124 **a collar flashed with the soil surface, representing the DEEP and SHAL treatments.**

125 We collected data between May and June of the 2021 dry season. Three chambers were rotated between the collars
126 on a near-weekly basis (periods 1-6; Table 1), ensuring that each period consisted of at least five full and
127 representative days. The fourth chamber was placed on an additional DEEP collar for the whole experiment
128 duration (the permanent type - PERM). The chambers were rotated in two configurations (Table 1): during periods
129 1, 3 and 5, each chamber was set over a different treatment, e.g., in period 1, chambers were placed over collars
130 CONV1, DEEP1, SHAL1; and during periods 2, 4 and 6, the three chambers were placed on the same treatment
131 (SAME), e.g., in period 2, chambers were placed over collars CONV1, CONV2, CONV3.

132

Table 1. Chamber placement during the 6 measurement periods - 12/05-29/06/2021

Period	1	2	3	4	5	6
Dates	12-18/05	18-22/05 27-30/05	30/05-03/06 06-09/06	09-16/06	16-22/06	24-29/06
Analyzed days	12-16/05	19-21/05 28-29/05	31/05-02/06 07-08/06	09-14/06	17-21/06	25-29/06
Treatment and replicate	CONV1 DEEP1 SHAL1	CONV 1-3	CONV2 DEEP2 SHAL2	DEEP 1-3	CONV3 DEEP3 SHAL3	SHAL 1-3

One chamber (PERM) continuously measured soil CO₂ flux on the same collar throughout the experiment.

133 2.4 Ancillary soil measurements

134 The temperature profile in the soil was measured by self-made T-type thermocouples buried at depths of 0.5, 1,
135 2, 3, 4, 5, 10, 15, 20, 30 and 50 cm. The thermocouple buried at 0.5 cm provided a proxy for the soil surface
136 temperature. The soil heat flux was derived using the combination method with three repetitions, using a soil heat

137 flux plate (HFT3, Campbell Scientific Inc.) buried at a depth of 5 cm. Heat storage above the plates was derived
138 from two self-made T-type thermocouples buried at depths of 1.25 and 3.75 cm, and soil water content was
139 measured with a time-domain reflectometer (TDR-315, Acclima, Inc., USA) installed at a depth of 3 cm. The
140 volumetric water content of the soil was lower than 3% throughout the experiment. Temperature profile and water
141 content data were collected at 10-second intervals, and 15-minute averages were stored in a data logger
142 (CR1000X, Campbell Scientific Inc.) and multiplexer (AM 16/32B, Campbell Scientific Inc.). Soil heat flux data
143 were also collected at 10-second intervals, and 15-minute averages were stored in a data logger (CR5000,
144 Campbell Scientific Inc.).

145 **2.5 Radiometric surface temperature**

146 A 24-hour field campaign was conducted on August 17-18, 2021. During the campaign, the surface radiometric
147 temperature of the collars was acquired hourly using a thermal infrared camera (A655sc, FLIR, Wilsonville,
148 USA), immediately before taking F_s measurements.

149 **2.6 Data analysis**

150 To calculate F_s , a linear function was fitted to the change in CO₂ mole fraction over time for each measurement,
151 using the software LI-COR SoilFluxPro 5.2.0 (LI-COR, Lincoln, USA). The fitting period, which usually lasted
152 20 seconds, started after air mixing within the chamber was achieved.

153 To decipher the differences between collars, and given the limited number of chambers, we derived an “average-
154 day” for each collar type (CONV, DEEP, and SHAL). First, five full representative days from each experiment
155 period (Table 1) were analyzed. Then, for each of the four chambers, an average diel course was calculated from
156 the 5 analyzed days, resulting in 4 average days per period. All average days from all periods (4 treatments × 6
157 periods= 24 average days) were then divided into 3 groups based on collar type (6 average days per treatment),
158 and a single average day per treatment was calculated as the mean of the 6 average days. Each time point in the
159 three treatment average days consists of 30 values (6 average days × 5 days per average).

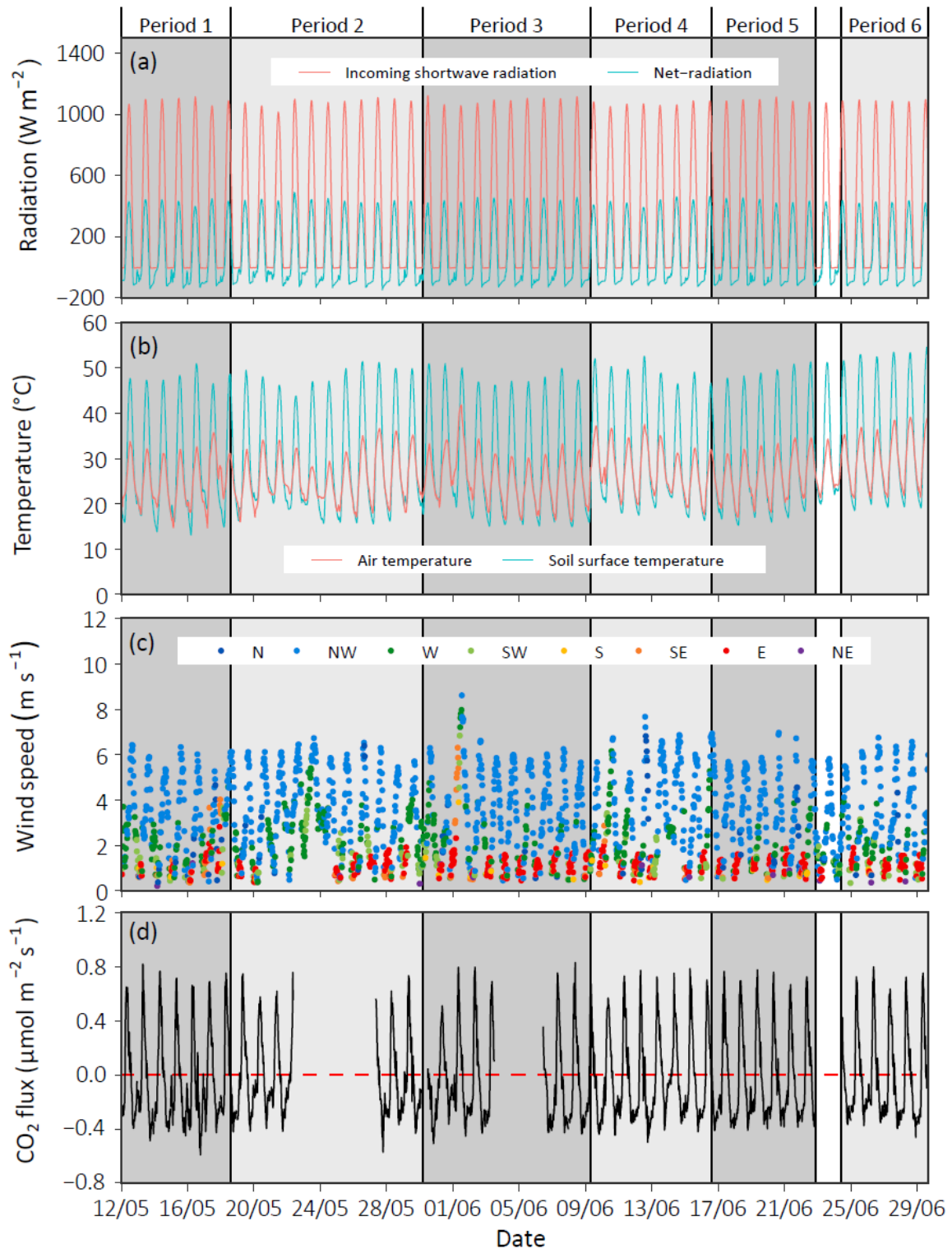
160 The differences between the treatments were tested for significance using linear mixed models (LMMs), following
161 the approach developed by Spyroglou et al. (2021). We built a statistical model Using LMMs that predicted the
162 response variable (i.e., the mean daily cycle of F_s) as a function of treatment and time as fixed factors (fixed for
163 all data points), and each collar as a subject-specific factor (random effect). This allowed us to assess the effect
164 of treatment, but also the effect of time and individual collars on F_s , while incorporating all 24-hour time series
165 into a single model. Still, this model fails to defuse the autocorrelation between data points in each time series. To
166 address this, the LMM residuals were passed through an Autoregressive Integrated Moving Average (ARIMA)
167 model and then incorporated within the LMM as errors. The predicted F_s values produced by the corrected model
168 were compared between treatments for each time interval separately using a two-tale t-test with a 95% confidence
169 interval. To avoid type I errors, the p-value was divided by the number of tests performed on each time point
170 according to the Bonferroni correction. Therefore, the corrected p-value used here is 0.05/6=0.008. The
171 differences between the treatments were also tested by comparing peak daily and daily accumulated efflux and
172 uptake value. This was executed using one-way ANOVA and a post hoc Tukey test with a 95% confidence
173 interval. The modeling process and statistical analysis were performed using “stats”, “lme4” and “forecast”
174 packages in RStudio 4.1.1.

175 To analyze the collars surface temperature, the region of interest (ROI) for each thermal image was defined for
176 the collar's inner surface area using FLIR ResearchIR Max 4.40.35. The surface temperature of all pixels within
177 the ROI were then exported to RStudio to calculate statistical parameters used to compare treatments. The soil
178 surface emissivity was set to 0.95 for all images (Li et al., 2013).

179 **3 Results**

180 **3.1 Meteorological and soil conditions**

181 The experiment period was characterized by clear sky days, with similar diel patterns and magnitudes of incoming
182 short-wave and net-radiation (Fig. 2). Solar noon occurred at 11:30 every day of the experiment (UTC+02:00).
183 Sunrise and sunset occurred at 04:30-05:00 and 19:00, respectively. The daily minimum and maximum air and
184 soil surface temperatures were 19.45 ± 2.3 and 34.5 ± 2.7 C° (air) and 17.7 ± 2 to 49.6 ± 2.2 C° (soil surface),
185 respectively. The mean daily range was 13.7 ± 1.0 and 31.8 ± 1.2 C°, for the air and the soil surface respectively,
186 with a slight variation between the experiment weeks. The soil surface temperature regularly dropped below air
187 temperature at night (Fig. 2B). The prevailing wind direction was NW, peaking in the afternoon at a mean speed
188 of 6.2 ± 0.2 m s⁻¹ (2 m height).



189

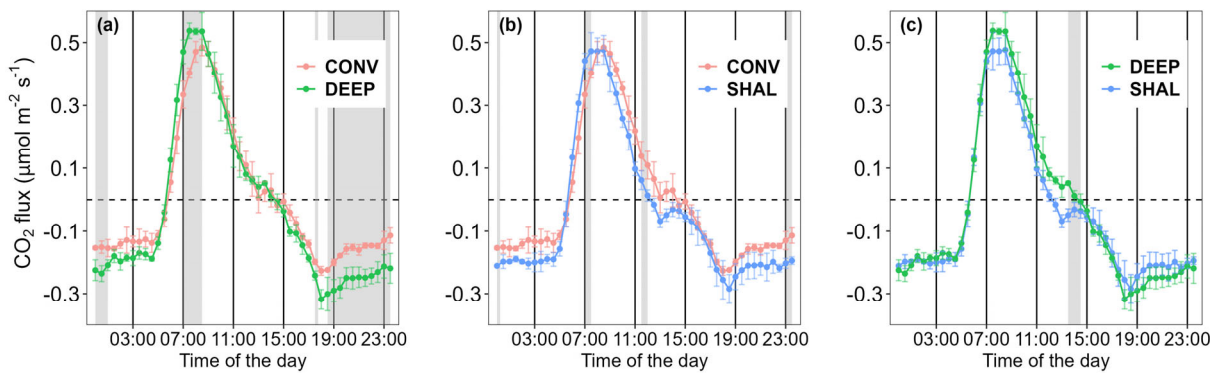
190 **Figure 2: Time series with half hourly data of environmental variables measured at the Wadi Mashash Experimental**
 191 **farm during the 2021 summer season. A) Incoming shortwave radiation and net radiation. B) Air and soil surface**
 192 **temperatures measured at 0.5 cm depth. C) Wind speed is color-coded according to wind direction: north (N), north-**
 193 **west (NW), west (W), south-west (SW), south (S), south-east (SE), east (E), and north-east (NE). D) The soil CO₂ flux**
 194 **measured by the permanent chamber (PHARM).**

195 Soil CO₂ flux measured on the permanent collar followed a consistent diurnal pattern throughout the experiment
 196 (Fig. 2d), confirming that the weekly periods can be used to test differences between treatments. Starting from the
 197 afternoon (mean time 13:30), negative CO₂ flux (i.e., uptake; from the atmosphere to the soil) occurred, peaking,

198 on average, at a flux of $-0.4 \pm 0.04 \mu\text{mol m}^{-2} \text{s}^{-1}$ (at 18:30). Then in the early morning (06:00), the flux reversed,
 199 and positive CO₂ flux (i.e., efflux; from the soil to the atmosphere) increased sharply until 08:30, when a daily
 200 maximum of $0.71 \pm 0.08 \mu\text{mol m}^{-2} \text{s}^{-1}$ was observed. After that, efflux gradually decreased until the afternoon.

201 3.2 The effect of collar type on soil CO₂ flux

202 The daily temporal dynamic of F_s shows little variation among the different treatments. However, the rate of
 203 increasing CO₂ efflux in the early morning, measured by the CONV collars, was lower than in the other treatments,
 204 as evidenced by the curve's concave nature (Fig. 3). Consequently, the daily maximum CO₂ efflux of CONV
 205 occurred at 08:30, an hour later than in the other treatments. The SHAL collars were also different from the other
 206 treatments in the timing of CO₂ uptake onset, occurring each day between 12:00-12:30, two hours before uptake
 207 started in the other treatments (Fig. 3).



208
 209 **Fig. 3. Mean daily cycles of the soil CO₂ flux measured in the following collar types- A) The conventional (CONV) and**
 210 **deep (DEEP) insertion types. B) The conventional (CONV) and shallow (SHAL) types. C) The shallow (SHAL) and**
 211 **deep (DEEP) types. Error bars denote two standard deviations (n=30). Gray areas represent periods in which**
 212 **differences between the treatments were statistically significant (p-value<0.008).**

213 The LMM model, combined with time series analysis, yielded statistically significant results ($P < 0.008$) for the
 214 differences in F_s between CONV and DEEP during the morning (07:00-08:30) and the evening/night (17:30-
 215 01:00). In fact, F_s of CONV were consistently lower than in DEEP. The relative differences peaked at 06:00 and
 216 23:30, when mean daytime CO₂ efflux and nocturnal CO₂ uptake were 56 and 53% lower in the CONV than in
 217 the DEEP. F_s measured in the CONV collars were also significantly lower than SHAL, by a maximum of 41%,
 218 but for shorter periods around noon and midnight. F_s measured in the DEEP collars were only significantly
 219 different from SHAL ($P < 0.008$) from 13:30 to 14:30.

220 The mean peak daily efflux measured in the DEEP treatment differed significantly from the other two treatments
 221 ($p < 0.05$), while no statistically significant difference in peak efflux was found for SHAL and CONV (one-way
 222 ANOVA and Tukey post hoc test). The differences between the total daily amount of CO₂ emitted during the day
 223 measured in SHAL and CONV were also insignificant ($p > 0.05$; Table 2). In contrast, the total daily amounts of
 224 CO₂ uptaken by the soil in the CONV collars were significantly lower than in the SHAL and the DEEP collars
 225 (Table 2), which may lead to erroneous estimations of daily net CO₂ exchange.

226

227

Table 2. Summary of main features- the mean daily cycles of *F_s*

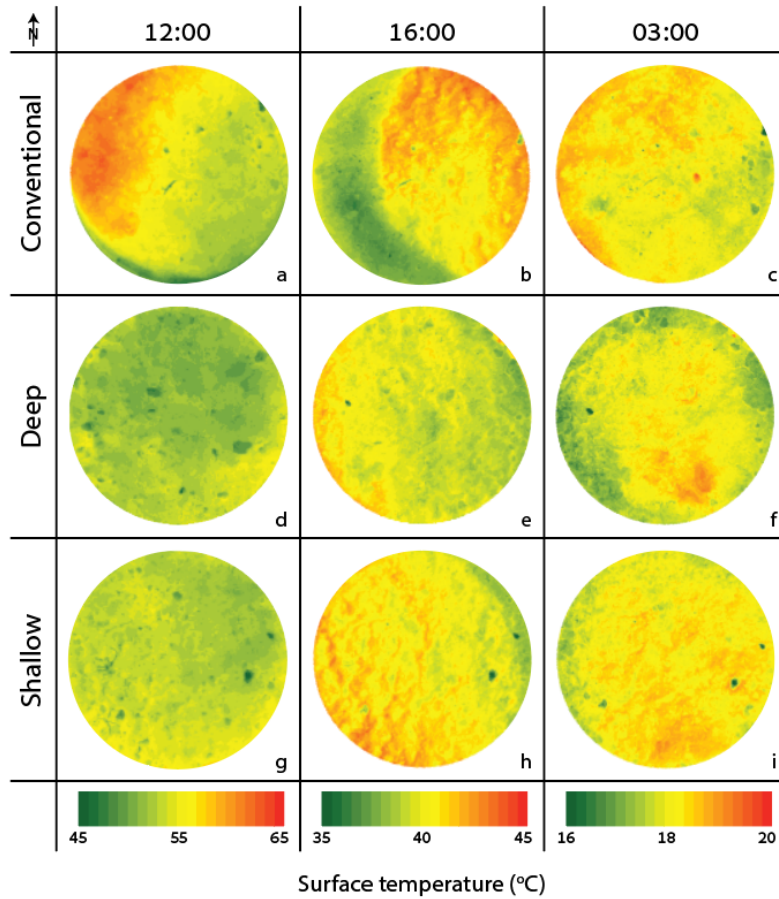
Period	Treatment	Max CO ₂ efflux	Max CO ₂ uptake	Total uptake	Total efflux
		$\mu\text{mol m}^{-2} \text{s}^{-1}$	$\mu\text{mol m}^{-2} \text{s}^{-1}$	g m^{-2}	g m^{-2}
1	CONV1	0.51±0.08	-0.28±0.04	0.43±0.077	0.29±0.04
	DEEP1	0.61±0.06	-0.38±0.05	0.54±0.05	0.39±0.06
	SHAL1	0.59±0.06	-0.38±0.06	0.57±0.10	0.32±0.05
2	CONV1	0.47±0.04	-0.26±0.03	0.30±0.05	0.33±0.04
	CONV2	0.51±0.06	-0.26±0.03	0.28±0.04	0.37±0.03
	CONV3	0.52±0.07	-0.27±0.02	0.31±0.06	0.32±0.04
3	CONV2	0.57±0.09	-0.25±0.04	0.36±0.11	0.39±0.04
	DEEP2	0.61±0.07	-0.36±0.03	0.53±0.13	0.34±0.09
	SHAL2	0.58±0.10	-0.35±0.03	0.49±0.12	0.33±0.08
4	DEEP1	0.64±0.08	-0.38±0.04	0.47±0.11	0.41±0.05
	DEEP2	0.67±0.11	-0.40±0.03	0.52±0.14	0.40±0.05
	DEEP3	0.57±0.10	-0.34±0.07	0.43±0.14	0.33±0.05
5	CONV3	0.55±0.04	-0.27±0.03	0.41±0.04	0.33±0.03
	DEEP3	0.60±0.01	-0.30±0.02	0.47±0.03	0.36±0.04
	SHAL3	0.48±0.04	-0.28±0.03	0.44±0.02	0.28±0.04
6	SHAL1	0.56±0.03	-0.32±0.01	0.46±0.11	0.34±0.01
	SHAL2	0.52±0.04	-0.28±0.03	0.37±0.08	0.28±0.03
	SHAL3	0.48±0.02	-0.27±0.02	0.35±0.09	0.29±0.03

228 Each value in the table is an average of 5 days \pm one standard deviation.

229

230 3.3 The effect of collar type on the radiometric soil surface temperature

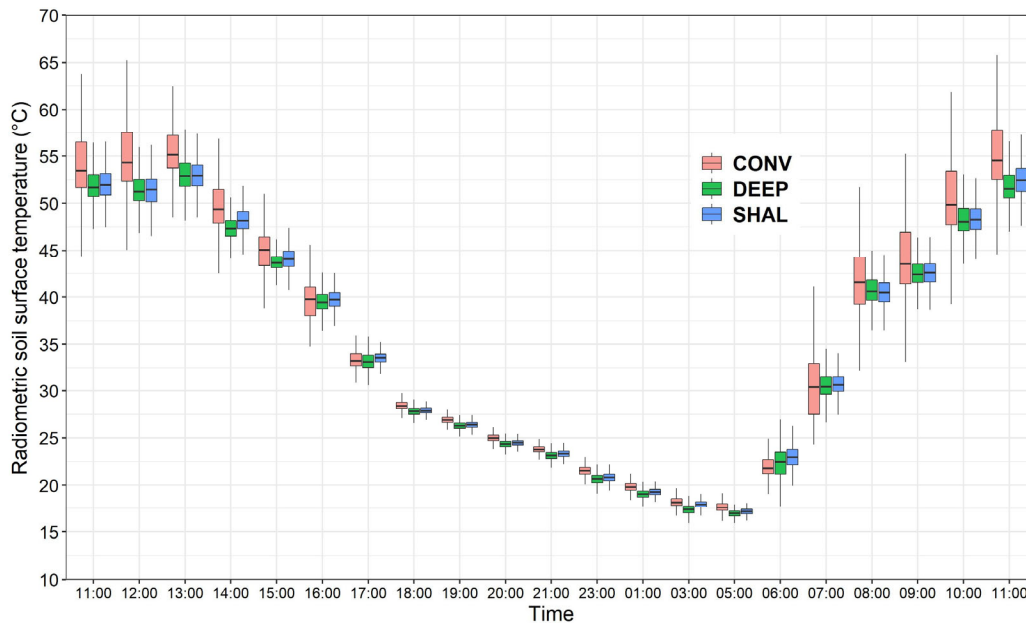
231 The mean and range of soil radiometric surface temperatures in the CONV collars were higher than in the DEEP
232 and SHAL collars, even at midday (Fig. 4). At 16:00, the three treatments all exhibited a mean surface temperature
233 of 40 °C, but the range of surface temperatures in the CONV collars doubled those of the other treatments. During
234 the night, the mean surface temperature of the CONV collars was 0.5-1 °C higher than in the DEEP collars and
235 0.5-0.9 °C higher than in the SHAL collars. After sunrise, the surface temperatures of the CONV and SHAL
236 increased faster than in the CONV collars up to 07:00. Later, the mean surface temperature of DEEP and SHAL
237 maintained a similar distribution over time, while the range and mean surface temperature in the CONV increased
238 sharply (Fig. 5).



239

240 **Figure 4: Thermal images of the soil surface radiometric temperature of one collar for each treatment in example hours**
 241 **of the day. A-C) The conventional treatment. D-F) The deep treatment. G-I) The shallow collar treatment. Note that**
 242 **each hour has a different temperature range.**

243

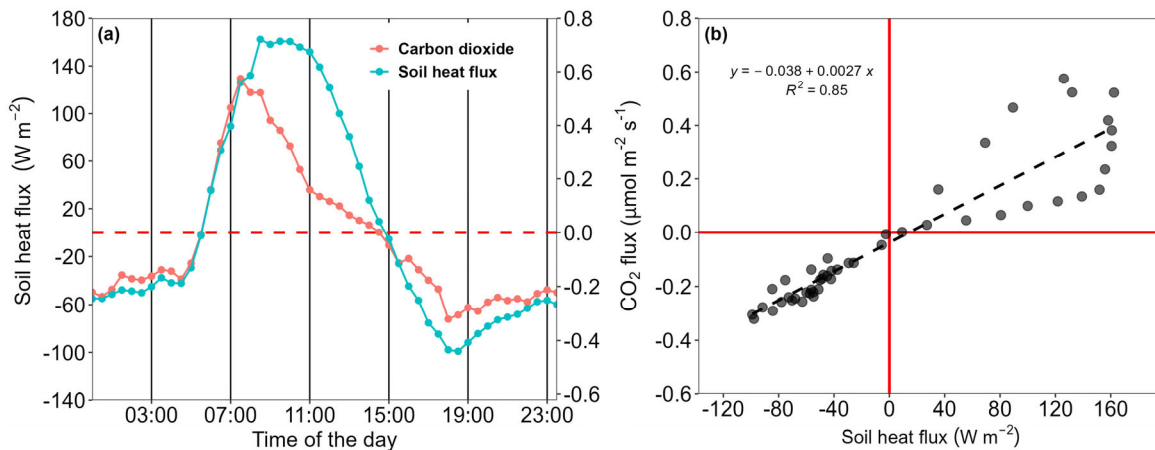


244

245 **Figure 5: Box plot and whiskers of the radiometric soil surface temperatures measured within the 3 types of collars on**
 246 **the 17-18/08/2021.**

247 **3.4 The effect of the soil heat flux on soil CO₂ flux**

248 Changes in soil surface temperature induced by the collar treatment significantly affected F_s . Nonetheless, F_s and
249 soil surface temperatures were uncoupled throughout the day and therefore may not be the sole variable that
250 explains F_s dynamics (Figs. 3 and 5). For example, while the soil surface temperature decreased throughout the
251 night, F_s decreased until the evening (18:00) and slowly increased during the night. However, the soil surface
252 temperature has a prime effect on the temperature profile within the soil, as well as the direction and magnitude
253 of soil heat flux. In fact, fig. 6 shows that F_s was linearly correlated with the soil heat flux, during the night and
254 morning efflux. Later, F_s decreased earlier than the soil heat flux, resulting in a daytime hysteresis relationship
255 (Fig. 6b).



256

257 **Figure 6: Relationship between the mean days of F_s and the soil heat flux for period 4 (9-16/06/2021). Note that positive**
258 **F_s values indicate that the direction of the flux is from the soil to the atmosphere and vice versa for negative F_s values.**
259 **Positive and negative soil heat flux values indicate the opposite directions than F_s values.**

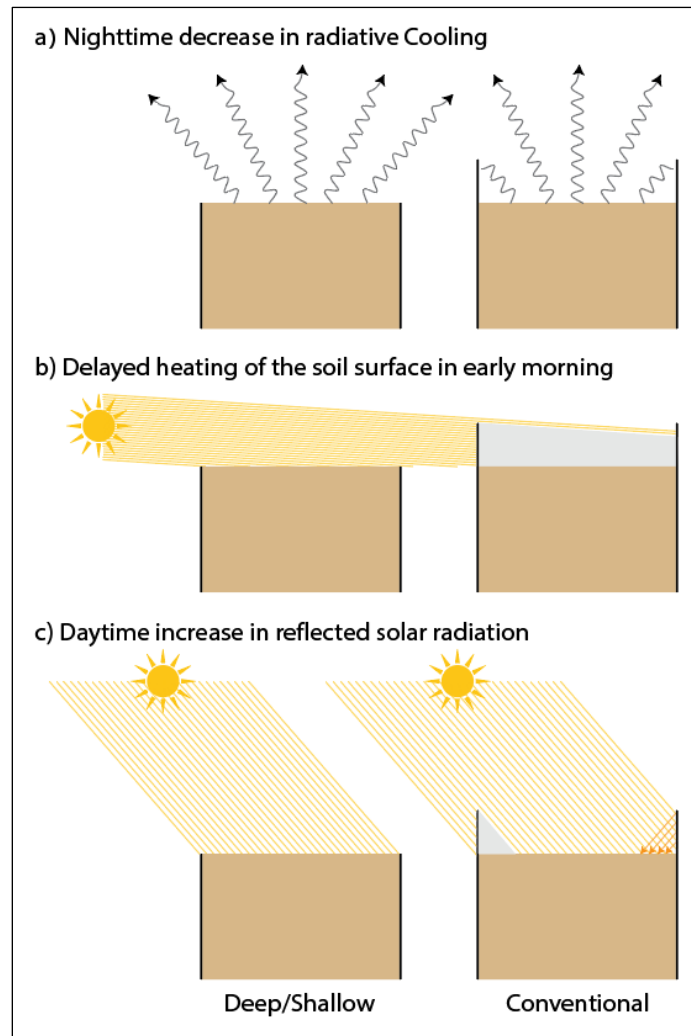
260 **4 Discussion**

261 Our study's results indicate that in dry and bare desert soils, using collars that protrude over the soil surface
262 (CONV) can decrease F_s . This finding is consistent with a prior global assessment that identified a negative
263 correlation between collar height above the soil surface and mean annual soil respiration rates (Jian et al., 2020).
264 However, while we found that protruding collars resulted in significant errors of nearly 50% in F_s (Fig. 3 and
265 table 2), Jian et al. (2020) demonstrated that collar height leads to a much smaller bias of only ~10% in annual
266 soil respiration rates. They explained this bias by nonuniform air mixing within the chamber system resulting
267 from the larger system volume but did not consider the potential effect of elevated collars on soil surface
268 temperatures. Moreover, 85% of the annual soil respiration rate values Jian et al. (2020) used were estimated
269 based on a limited number of instantaneous CO₂ efflux measurements, which were usually performed during the
270 daytime, and, therefore, overlook diurnal dynamics in F_s . Since F_s is not constant throughout the day in desert
271 soils but varies between daytime efflux and nocturnal uptake (Fig. 3), a small discontinuous number of daytime
272 measurements will fail to capture errors in flux measurements. Finally, while most studies discussing potential
273 sources of errors in F_s measurements were conducted in conditions where the dominant flux is a result of microbial
274 respiration, in dry desert soils F_s is primarily driven by an abiotic process governed by changes in soil temperatures
275 (Soper et al., 2017). Therefore, errors associated with using static chambers in dry desert soils are likely related

276 to alteration of geochemical processes in the soil rather than affecting the factors that influence soil microbial
277 activity.

278 The abiotic process driving nocturnal CO₂ uptake in desert soils is often explained by the combined effect of
279 contraction and dissolution of gaseous CO₂ in soil water. These processes decrease gaseous CO₂ concentration in
280 the soil surface layer, forming an atmosphere-to-soil concentration gradient and CO₂ diffusion into the soil (Yang
281 et al., 2020; Sagi et al., 2021). Contraction of soil air may decrease CO₂ concentration in the soil surface layer and
282 lead to atmosphere-to-soil pressure gradient and thermal convection, which further contributes to CO₂ uptake
283 (Ganot et al., 2014). Soil temperature negatively affects both contraction and dissolution. Higher temperature
284 result in less contraction and dissolution, thus a higher CO₂ concentration in the surface air-filled soil-pores,
285 ultimately leading to a smaller soil-atmosphere CO₂ gradient, and lower F_s . [It is therefore expected that a
286 modification of the surface temperature by the collar will affect the magnitude of the flux.](#)

287 The elevated walls in the CONV collars limit nocturnal radiative cooling of the topsoil layer, resulting in higher
288 soil temperatures that suppress the CO₂ concentration gradient and the actual CO₂ uptake from the atmosphere
289 (Fig. 4 and fig. 7). Following sunrise, soil temperature increases in the DEEP and SHAL collars, promoting CO₂
290 expansion and outgassing from water films, rapidly increasing CO₂ efflux (Fa et al., 2016). This process is delayed
291 in the CONV collars because the surface is entirely shaded by the collar walls (Fig. 7b), resulting in a lower mean
292 temperature and a narrower overall range of surface temperatures (Fig. 5; 06:00 and Fig. 7b). As a result, CO₂
293 efflux increases at a slower rate (Fig. 3). When the sun elevation increases, solar radiation is reflected off the
294 collar walls into the measured area, increasing the radiation flux in the unshaded soil surface and, consequently,
295 increasing the mean and range of soil surface temperatures compared to the DEEP and SHAL collars (Figs. 4A-
296 B, 5 and 7). Thus, lower surface temperatures cannot explain the significantly lower CO₂ efflux measured in the
297 CONV collars between 07:00 and 08:30. Instead, it is probably related to the significantly lower total nighttime
298 CO₂ uptake, which leads to a faster depletion of soil CO₂ in the following morning (Table 2).



299
300
301

Figure 7: Conceptual model showing the effects of collar deployment on soil surface radiative heating and cooling during the night (a), early morning (b), and daytime (c).

302

303 The results of our study indicate that lateral diffusion is not a significant concern in dry, bare desert soils when
 304 the measurement period (i.e., the length of time during which the chamber is closed over the collar) is short, as
 305 demonstrated by the insignificant differences between F_s measured over the SHAL and DEEP collars. This
 306 confirms the findings of Hutchinson and Livingston, (2001). Although statistically insignificant, the mean CO_2
 307 efflux in the SHAL collars was consistently lower than in the DEEP collars between 7:00 and 14:30 (Fig. 3 and
 308 table 2). Additionally, the flux direction measured over the SHAL collars, consistently changed from efflux
 309 (positive) to uptake (negative) earlier than in the other treatments, and earlier than the soil heat flux changed from
 310 positive to negative (Fig. 6). A change in the soil heat flux sign indicates that temperatures in the uppermost soil
 311 layer are decreasing, promoting the removal of gaseous CO_2 from the soil air phase, followed by CO_2 uptake from
 312 the atmosphere. Hence, when soil temperatures are undisturbed (e.g., by the presence of a collar), we expect the
 313 onset of CO_2 uptake to coincide with the change in soil heat flux direction (Fig. 6). The only difference between
 314 the SHAL and DEEP collars was their insertion depth (in both the collar's top end was flashed with the soil
 315 surface). Root cutting, which is often suggested as an explanation for lower F_s measured over deeper collars
 316 (Heinemeyer et al., 2011), is inapplicable when the soil is sparsely vegetated. Furthermore, our results show higher
 317 F_s values when measured over deeply inserted collars (DEEP) then when measured over shallow collars (SHAL).

318 Potential overestimation of F_s resulting from enhanced air flow along the collar walls in the DEEP collars was
319 minimized by inserting the collars more than two months prior the measurements, a sufficiently long time to allow
320 the soil to settle around them (Hutchinson and Livingston, 2001). Lateral diffusion below the shallow collars
321 therefore remains the most probable explanation. As suggested by Healy et al. (1996), lateral movement likely
322 decreased the CO₂ concentration in the soil top layer during CO₂ efflux, decreasing the concentration gradient
323 between the soil and the chamber headspace, resulting in an underestimation of F_s . The lower soil CO₂
324 concentration beneath the SHAL collars caused the concentration gradient that drives the vertical flux to reverse
325 direction toward the soil, starting CO₂ uptake earlier than in the other treatments (fig. 3).

326 The conventionally deployed collars (CONV) underestimated the instantaneous CO₂ uptake and thus the total CO₂
327 uptake during the night (table 2). This suggests that the actual carbon sequestration by desert soils is higher than
328 previously reported. In some cases, the net daily exchange measured in the CONV collars is even positive,
329 indicating a net efflux of CO₂ to the atmosphere (Table 2). Note, however, that the net daily values measured by
330 the CONV collars are very small, thus more susceptible to errors, to the point of flipping the direction, and
331 concluding from the absolute daily net values must be done with caution. Theoretically, if F_s in dry desert soils is
332 derived by abiotic geochemical processes, a balanced net daily cycle would be expected, where nocturnal CO₂
333 uptake is compensated by daytime efflux. Even in alkaline soils, such as the ones in our study site, where the
334 nocturnal dissolution of CaCO₃ may sustain CO₂ uptake from the atmosphere, the reverse reaction should occur
335 when water evaporates and CaCO₃ precipitates, promoting CO₂ efflux and system equilibrium (Roland et al.,
336 2013). This hypothesis was supported by Hamerlynck et al. (2013) who found that a soil in the Chihuahuan Desert,
337 USA, only serves as a minor carbon sink (0.88 g C m⁻² accumulated over three months) and concluded that this
338 contribution is insignificant to the global carbon balance. Contrarily, in the Taklamakan (Yang et al., 2020) and
339 the Gubantonggut (Xie et al., 2009) Deserts in China, nocturnal CO₂ uptake led to a mean annual uptake of 7.11
340 and 62-622 g C m⁻², respectively. This gave rise to the hypothesis that nocturnal CO₂ uptake by desert soils might
341 explain a substantial portion of the global missing sink. However, they did not provide a mechanism to explain
342 where the carbon is stored, especially given that the leaching of dissolved carbonates to groundwater is limited in
343 space and time (Ma et al., 2014; Schlesinger, 2017; Yang et al., 2022). Furthermore, the abiotic component of F_s
344 contributed 21% of mean CO₂ efflux in a semi-arid pine forest located ~35 km north-east of near our study site
345 and therefor functioned as a source for atmospheric carbon rather than as a sink in that ecosystem (Qubaja et al.,
346 2020). Either way, no conclusions can be drawn about the role desert soils play in the missing sink global carbon
347 balance until a methodology to measure these small fluxes is proved to be accurate. Our study shows that
348 instantaneous F_s and F_s daily balance could be significantly affected by even as small as a few centimeters
349 difference in collar height and depth. This implies that previous estimates of the carbon balance of desert
350 ecosystems using static chambers need to be carefully considered.

351 In fact, studies show that the abiotic mechanisms involved in F_s are not restricted to dry desert conditions but
352 rather play a significant role in F_s in deserts under wet soil conditions (Fa et al., 2016). This was found for both a
353 semi-arid pine forest (Qubaja et al., 2020), and a temperate grassland (Plestenjak et al., 2012). Hence, the collar
354 disruption to abiotic processes likely affects the carbon balance in various ecosystems beyond the scope of deserts
355 during the dry season. Alteration of F_s due to collar insertion is not restricted to abiotic processes. The soil
356 biological processes, and specially activity of biological soil crust, may be significantly affected by altered soil

357 surface conditions. Since they cover a vast area of Earth's drylands, and play a significant role in desert
358 ecosystem's carbon balance (Wilske et al., 2008), it is important to consider these effects.

359 **5 Summary and Conclusions**

360 The drivers of abiotic soil CO₂ flux observed in dry desert soils are yet far from being understood. Further research
361 is needed to reconcile the discrepancy between the theoretical basis, which suggests a balanced daily cycle, and
362 field measurements, which often show net uptake by the soil in both diel and annual scales. Particularly, studies
363 should focus on improving our understanding of CO₂ in the soil profile in desert soils, and on allocating the
364 sources of water that are assumed to act as a solvent for CO₂ even when the soil is dry. None of these questions,
365 however, can be addressed without an accurate methodology to measure the small F_s characterizing bare desert
366 soils.

367 During a two months measurement period in the summer of 2021, the soil in the Wadi Mashash Experimental
368 farm exhibited a repetitive diel cycle of CO₂ flux that consisted of nocturnal CO₂ uptake and daytime efflux,
369 driven by a combination of physical and geochemical processes in the soil. We show here for the first time that
370 collar deployment practices significantly affect this abiotic diel cycle by altering the factors that drive F_s . Notably,
371 morning CO₂ efflux and nocturnal CO₂ uptake were underestimated when measured on conventionally inserted
372 collars because the elevated collar walls distorted the ambient surface temperature regime. We conclude that in
373 bare desert soils collars should be deployed flush with the soil surface to prevent distortion of heat exchange
374 between the soil and the atmosphere and between soil layers, two important drivers of the abiotic F_s . Lateral
375 diffusion under shallow collars may occur and affect F_s ' temporal dynamics. However, we found this to be of a
376 lesser concern in compact soils and short measurement periods. Still, in dry desert soils, the collar insertion depth
377 should exceed the depth at which the fluctuations in soil CO₂ concentration that drive F_s occur, roughly 2 cm
378 (Hamerlynck et al., 2013).

379 Deployment protocols of flux chambers should be adapted to the unique characteristics of desert soils rather than
380 follow standard procedures suitable for mesic environments. We conclude that using collars with at least 3 cm
381 length inserted flush with the soil surface will minimize measurement errors of CO₂ flux and will pave the way to
382 accurate estimates of the carbon balance of desert ecosystems.

383 **6 Code/data availability**

384 Code and data will be provided upon request.

385 **7 Author contributions**

386 **Nadav Bekin:** Conceptualization, Data curation, Formal analysis, Investigation, Methodology, Writing - original
387 draft. **Nurit Agam:** Conceptualization, Funding acquisition, Methodology, Project administration, Resources,
388 Supervision, Writing - review & editing.

389 **8 Competing interests**

390 The authors have no competing interests.

391 **9 Acknowledgments**

392 This research was supported by the Israel Science Foundation (grant number 2381/21).

393 **10 References**

394 Austin, A. T., Yahdjian, L., Stark, J. M., Belnap, J., Porporato, A., Norton, U., Ravetta, D. A., and Schaeffer, S.
395 M.: Water pulses and biogeochemical cycles in arid and semiarid ecosystems, *Oecologia*, 141, 221–235,
396 <https://doi.org/10.1007/s00442-004-1519-1>, 2004.

397 Bain, W. G., Hutyra, L., Patterson, D. C., Bright, A. V., Daube, B. C., Munger, J. W., and Wofsy, S. C.: Wind-
398 induced error in the measurement of soil respiration using closed dynamic chambers, *Agric. For. Meteorol.*, 131,
399 225–232, <https://doi.org/10.1016/j.agrformet.2005.06.004>, 2005.

400 Ball, B. A., Virginia, R. A., Barrett, J. E., Parsons, A. N., and Wall, D. H.: Interactions between physical and
401 biotic factors influence CO₂ flux in Antarctic dry valley soils, *Soil Biol. Biochem.*, 41, 1510–1517,
402 <https://doi.org/10.1016/j.soilbio.2009.04.011>, 2009.

403 Baram, S., Bar-Tal, A., Gal, A., Friedman, S. P., and Russo, D.: The effect of static chamber base on N₂O flux in
404 drip irrigation, *Biogeosciences*, 19, 3699–3711, <https://doi.org/10.5194/bg-19-3699-2022>, 2022.

405 Brutsaert, W.: Evaporation into the Atmosphere, <https://doi.org/10.1007/978-94-017-1497-6>, 1982.

406 Cable, J. M., Ogle, K., Williams, D. G., Weltzin, J. F., and Huxman, T. E.: Soil texture drives responses of soil
407 respiration to precipitation pulses in the sonoran desert: Implications for climate change, *Ecosystems*, 11, 961–
408 979, <https://doi.org/10.1007/s10021-008-9172-x>, 2008.

409 Cable, J. M., Ogle, K., Lucas, R. W., Huxman, T. E., Loik, M. E., Smith, S. D., Tissue, D. T., Ewers, B. E.,
410 Pendall, E., Welker, J. M., Charlet, T. N., Cleary, M., Griffith, A., Nowak, R. S., Rogers, M., Steltzer, H., Sullivan,
411 P. F., and van Gestel, N. C.: The temperature responses of soil respiration in deserts: A seven desert synthesis,
412 *Biogeochemistry*, 103, 71–90, <https://doi.org/10.1007/s10533-010-9448-z>, 2011.

413 Fa, K., Zhang, Y., Lei, G., Wu, B., Qin, S., Liu, J., Feng, W., and Lai, Z.: Underestimation of soil respiration in a
414 desert ecosystem, *Catena*, 162, 23–28, <https://doi.org/10.1016/j.catena.2017.11.019>, 2018.

415 Fa, K. Y., Zhang, Y. Q., Wu, B., Qin, S. G., Liu, Z., and She, W. W.: Patterns and possible mechanisms of soil
416 CO₂ uptake in sandy soil, *Sci. Total Environ.*, 544, 587–594, <https://doi.org/10.1016/j.scitotenv.2015.11.163>,
417 2016.

418 Ganot, Y., Dragila, M. I., and Weisbrod, N.: Impact of thermal convection on CO₂ flux across the earth-
419 atmosphere boundary in high-permeability soils, *Agric. For. Meteorol.*, 184, 12–24,
420 <https://doi.org/10.1016/j.agrformet.2013.09.001>, 2014.

421 Hamerlynck, E. P., Scott, R. L., Sánchez-Cañete, E. P., and Barron-Gafford, G. A.: Nocturnal soil CO₂ uptake
422 and its relationship to subsurface soil and ecosystem carbon fluxes in a Chihuahuan Desert shrubland, *J. Geophys.*
423 *Res. Biogeosciences*, 118, 1593–1603, <https://doi.org/10.1002/2013JG002495>, 2013.

424 Healy, R. W., Striegl, R. G., Russell, T. F., Hutchinson, G. L., and Livingston, G. P.: Numerical Evaluation of
425 Static-Chamber Measurements of Soil-Atmosphere Gas Exchange: Identification of Physical Processes, *Soil Sci.*
426 *Soc. Am. J.*, 60, 740–747, <https://doi.org/10.2136/sssaj1996.03615995006000030009x>, 1996.

427 Heinemeyer, A., Di Bene, C., Lloyd, A. R., Tortorella, D., Baxter, R., Huntley, B., Gelsomino, A., and Ineson,
428 P.: Soil respiration: Implications of the plant-soil continuum and respiration chamber collar-insertion depth on
429 measurement and modelling of soil CO₂ efflux rates in three ecosystems, *Eur. J. Soil Sci.*, 62, 82–94,
430 <https://doi.org/10.1111/j.1365-2389.2010.01331.x>, 2011.

431 Houghton, R. A.: Balancing the global carbon budget, *Annu. Rev. Earth Planet. Sci.*, 35, 313–347,
432 <https://doi.org/10.1146/annurev.earth.35.031306.140057>, 2007.

433 Jian, J., Gough, C., Sihi, D., Hopple, A. M., and Bond-Lamberty, B.: Collar Properties and Measurement Time
434 Confer Minimal Bias Overall on Annual Soil Respiration Estimates in a Global Database, *J. Geophys. Res.*
435 *Biogeosciences*, 125, 1–13, <https://doi.org/10.1029/2020JG006066>, 2020.

436 Li, Z. L., Wu, H., Wang, N., Qiu, S., Sobrino, J. A., Wan, Z., Tang, B. H., and Yan, G.: Land surface emissivity
437 retrieval from satellite data, *Int. J. Remote Sens.*, 34, 3084–3127, <https://doi.org/10.1080/01431161.2012.716540>,
438 2013.

439 Lopez-Canfin, C., Lázaro, R., and Sánchez-Cañete, E. P.: Water vapor adsorption by dry soils: A potential link
440 between the water and carbon cycles, *Sci. Total Environ.*, 824, <https://doi.org/10.1016/j.scitotenv.2022.153746>,
441 2022.

442 Lund, C. P., Riley, W. J., Pierce, L. L., and Field, C. B.: The effects of chamber pressurization on soil-surface
443 CO₂ flux and the implications for NEE measurements under elevated CO₂, *Glob. Chang. Biol.*, 5, 269–281,
444 <https://doi.org/10.1046/j.1365-2486.1999.00218.x>, 1999.

445 Ma, J., Liu, R., Tang, L. S., Lan, Z. D., and Li, Y.: A downward CO₂ flux seems to have nowhere to go,
446 *Biogeosciences*, 11, 6251–6262, <https://doi.org/10.5194/bg-11-6251-2014>, 2014.

447 Ngao, J., Longdoz, B., Perrin, D., Vincent, G., Epron, D., Le Dantec, V., Soudani, K., Aubinet, M., Willim, F.,
448 and Granier, A.: Cross-calibration functions for soil CO₂ efflux measurement systems, *Ann. For. Sci.*, 63, 477–
449 484, <https://doi.org/10.1051/forest:2006028>, 2006.

450 Ninari, N. and Berliner, P. R.: The role of dew in the water and heat balance of bare loess soil in the Negev Desert:
451 Quantifying the actual dew deposition on the soil surface, *Atmos. Res.*, 64, 323–334,
452 [https://doi.org/10.1016/S0169-8095\(02\)00102-3](https://doi.org/10.1016/S0169-8095(02)00102-3), 2002.

453 Parkin, T. B., Venterea, R. T., and Hargreaves, S. K.: Calculating the Detection Limits of Chamber-based Soil
454 Greenhouse Gas Flux Measurements, *J. Environ. Qual.*, 41, 705–715, <https://doi.org/10.2134/jeq2011.0394>, 2012.

455 Parsons, A. N., Barrett, J. E., Wall, D. H., and Virginia, R. A.: Soil Carbon Dioxide Flux in Antarctic Dry Valley

456 Ecosystems, *Ecosystems*, 286–295, <https://doi.org/10.1007/s10021-003-0132-1>, 2004.

457 Plestenjak, G., Eler, K., and Vodnik, D.: Sources of soil CO₂ in calcareous grassland with woody plant
458 encroachment, *J. soils sediments*, 1327–1338, <https://doi.org/10.1007/s11368-012-0564-3>, 2012.

459 Pumpanen, J., Kolari, P., Ilvesniemi, H., Minkkinen, K., Vesala, T., Niinistö, S., Lohila, A., Larmola, T., Morero,
460 M., Pihlatie, M., Janssens, I., Yuste, J. C., Grünzweig, J. M., Reth, S., Subke, J. A., Savage, K., Kutsch, W.,
461 Østreng, G., Ziegler, W., Anthoni, P., Lindroth, A., and Hari, P.: Comparison of different chamber techniques for
462 measuring soil CO₂ efflux, *Agric. For. Meteorol.*, 123, 159–176,
463 <https://doi.org/10.1016/j.agrformet.2003.12.001>, 2004.

464 Pumpanen, J., Longdoz, B., and Kutsch, W. L.: Field measurements of soil respiration: Principles and constraints,
465 potentials and limitations of different methods, *Soil Carbon Dyn. An Integr. Methodol.*, 16–33,
466 <https://doi.org/10.1017/CBO9780511711794.003>, 2010.

467 Qubaja, R., Tatarinov, F., Rotenberg, E., and Yakir, D.: Partitioning of canopy and soil CO₂ fluxes in a pine
468 forest at the dry timberline across a 13-year observation period, *Biogeosciences*, 4, 699–714, 2020.

469 Rochette, P. and Eriksen-Hamel, N. S.: Chamber Measurements of Soil Nitrous Oxide Flux: Are Absolute Values
470 Reliable?, *Soil Sci. Soc. Am. J.*, 72, 331–342, <https://doi.org/10.2136/sssaj2007.0215>, 2008.

471 Roland, M., Serrano-Ortiz, P., Kowalski, A. S., Goddérís, Y., Sánchez-Cañete, E. P., Ciais, P., Domingo, F.,
472 Cuezva, S., Sanchez-Moral, S., Longdoz, B., Yakir, D., Van Grieken, R., Schott, J., Cardell, C., and Janssens, I.
473 A.: Atmospheric turbulence triggers pronounced diel pattern in karst carbonate geochemistry, *Biogeosciences*, 10,
474 5009–5017, <https://doi.org/10.5194/bg-10-5009-2013>, 2013.

475 Sagi, N., Zaguri, M., and Hawlena, D.: Soil CO₂ influx in drylands: A conceptual framework and empirical
476 examination, *Soil Biol. Biochem.*, 156, 108209, <https://doi.org/10.1016/j.soilbio.2021.108209>, 2021.

477 Soper, F. M., McCalley, C. K., Sparks, K., and Sparks, J. P.: Soil carbon dioxide emissions from the Mojave
478 desert: Isotopic evidence for a carbonate source, *Geophys. Res. Lett.*, 44, 245–251,
479 <https://doi.org/10.1002/2016GL071198>, 2017.

480 Spyroglou, I., Skalák, J., Balakhonova, V., Benedikty, Z., Rigas, A. G., and Hejátko, J.: Mixed models as a tool
481 for comparing groups of time series in plant sciences, *Plants*, 10, 1–16, <https://doi.org/10.3390/plants10020362>,
482 2021.

483 Stell, E., Warner, D., Jian, J., Bond-Lamberty, B., and Vargas, R.: Spatial biases of information influence global
484 estimates of soil respiration: How can we improve global predictions?, *Glob. Chang. Biol.*, 27, 3923–3938,
485 <https://doi.org/10.1111/gcb.15666>, 2021.

486 Wilske, B., Burgheimer, J., Karnieli, A., Zaady, E., Andreae, M. O., Yakir, D., and Kesselmeier, J.: The CO₂
487 exchange of biological soil crusts in a semiarid grass-shrubland at the northern transition zone of the Negev desert
488 , Israel, *Biogeosciences*, 1411–1423, 2008.

489 Xie, J., Li, Y., Zhai, C., Li, C., and Lan, Z.: CO₂ absorption by alkaline soils and its implication to the global
490 carbon cycle, *Environ. Geol.*, 56, 953–961, <https://doi.org/10.1007/s00254-008-1197-0>, 2009.

491 Yang, F., Huang, J., He, Q., Zheng, X., Zhou, C., Pan, H., Huo, W., Yu, H., Liu, X., Meng, L., Han, D., Ali, M.,
492 and Yang, X.: Impact of differences in soil temperature on the desert carbon sink, *Geoderma*, 379, 114636,
493 <https://doi.org/10.1016/j.geoderma.2020.114636>, 2020.

494 Yang, F., Huang, J., Zheng, X., Huo, W., Zhou, C., Wang, Y., Han, D., Gao, J., Mamtimin, A., Yang, X., and
495 Sun, Y.: Evaluation of carbon sink in the Taklimakan Desert based on correction of abnormal negative CO₂ flux
496 of IRGASON, *Sci. Total Environ.*, 838, 155988, <https://doi.org/10.1016/j.scitotenv.2022.155988>, 2022.

497

498

499